JOURNAL OF PROPULSION AND POWER
Vol. 24, No. 4, July–August 2008

Hydrocarbon Fuel Flash Vaporization for Pulsed Detonation Combustion

K. Colin Tucker*
U.S. Air Force Research Laboratory, Eglin Air Force Base, Florida 32542
Paul I. King†
Air Force Institute of Technology, Wright–Patterson Air Force Base, Ohio 45433
and
Frederick R. Schauer‡
U.S. Air Force Research Laboratory, Wright–Patterson Air Force Base, Ohio 45433

DOI: 10.2514/1.28412

Practical operation of pulsed detonation propulsion requires operation on kerosene-based jet fuels. These low vapor pressure fuels remain in liquid form at typical pulsed detonation inlet conditions and residence times, and the subsequent presence of fuel droplets significantly slows the combustion and hinders engine operability. A fuel flash vaporization system was designed and built to reduce evaporation time and provide gaseous fuel to the pulsed detonation engine. Four fuels that vary in volatility were tested: n-heptane, isooctane, aviation gasoline, and JP-8. Results showed the flash vaporization system quickly provides a detonable mixture for all of the fuels tested without coking the fuel lines. A significant result of this work was the successful detonation of flash vaporized JP-8 in air over a range of fuel temperatures and fuel-to-air ratios.

Introduction

THE pulsed detonation engine (PDE) is an attractive propulsion system for military use because of its simplicity, low cost, and potential for large flight Mach numbers (0–5) [1,2]. Some difficulties in the development of the PDE have been in creating a droplet-free fuel and air mixture quickly enough and initiating or transitioning detonations at a high enough frequency to create practical thrust levels with liquid-fuel systems [3]. The available time to provide an adequate fuel/air mixture is typically on the order of milliseconds and depends on both the cycle rate and the mixing length dictated by the engine geometry. The presence of droplets in a fuel–air mixture have been shown to negatively affect ignition, deflagration to detonation transition (DDT), and detonation wave propagation through the mixture [4–8]. In a typical high-pressure fuel liquid injection system (without flash vaporization), pressure atomization nozzles can generate droplets roughly 20–70 μm in size.§ When mixed with moderately heated air, the fuel droplets will evaporate after some finite time, significant relative to the cycle period. Because the PDE operates on a cycle where detonative combustion is repeatedly initiated to produce thrust, the time required to detonate the fuel and air mixture is crucial. If fuel droplets remain, some of the ignition energy is consumed in evaporating the liquid, thus slowing ignition and the amount of fuel vapor available for combustion. Kailasanath noted in his review [9] that if low vapor pressure fuels had droplets smaller than 10 μm then the effects of the droplets were negligible in the propagation of a detonation, assuming there was sufficient fuel vapor available to initiate combustion. Prior efforts [10] showed that, to avoid inhibiting combustion, the final mixture of air and fuel (for low vapor pressure JP-8) must be above about 400 K for the mixing process to completely evaporate the fuel in a 1.3 m long manifold at 2 bar. A solution discussed in this paper is the use of a precombustion flash vaporization system (FVS) to raise the enthalpy of the fuel before air mixing, such that no energy is required from the air to evaporate the droplets and provide the PDE a droplet-free, homogeneous fuel/air mixture.

Heating hydrocarbon fuels to high temperatures is not without certain problems. At flash vaporization temperatures, oxygen dissolved in the fuel can react to induce deposition of carbon and cause other problems within the fuel system. In the earliest documented flash vaporization system [11], Whittle heated fuel above the boiling point in a gas turbine combustor, but poor fuel flow control and clogged fuel lines hindered efficient combustion. The clogged fuel lines were due to thermal oxidation and endothermic reactions: reactions that have since delayed the implementation of practical flash vaporization systems.

Observable thermal oxidation reaction rates begin at fuel temperatures between 393 and 533 K [12]. The products from these reactions cause carbon particulates and carbonaceous deposits on metal surfaces in fuel systems that clog spray nozzles and cake on tubing walls. Depositions increase with increased dissolved oxygen in the fuel and with increased fuel temperature. Thermal oxidation reactions can be suppressed up to approximately 750 K by reducing the oxygen content to less than 1 ppm [12].

Endothermic reactions (due to cracking) also produce particulates and clog fuel lines. Cracking percentage, though, is highly dependent on soak time at high temperatures. Yoon et al. [13] showed that N_2-deoxygenated n-dodecane (n-$C_{12}H_{26}$) decomposed by 20% in about 4 h at 400°C, but, at 450°C, the fuel decomposed 20% in only 17 min. For the flash vaporization system described in this work, the fuel was statically heated before use to temperatures up to 350°C. In flowing systems, low residence, and thus low soak times, allow for higher fuel temperatures without cracking the fuel. Ward et al. [14] sustained no measurable cracking of flowing n-dodecane (n-$C_{12}H_{26}$) with a wall temperature of 500°C. Ervin et al. [12] heated flowing deoxygenated Jet A near 480°C before significant cracking occurred.

To prevent thermal-oxidative reactions in this work, dissolved oxygen was removed by sparging the fuel with nitrogen before pressurization and heating. Sparging consists of bubbling gaseous nitrogen through ambient temperature liquid fuel to agitate and

---

Received 19 October 2006; accepted for publication 6 February 2008.

[*] Major, Munitions Directorate, 101 W. Eglin Blvd. Senior Member AIAA.

[†] Professor, Department of Aeronautics and Astronautics, 2950 Hobson Way. Senior Member AIAA.

[‡] Research Engineer, Propulsion Directorate, 1790 Loop Road. Senior Member AIAA.

[§] Data supplied by Goodrich Turbine Fuel Technologies, West Des Moines, IA.

Table 1 Fuel vapor pressures (kPa) at various temperatures from [15–17]

Temperature, °C	Isooctane	N-heptane	Aviation gasoline	JP-8	JP-10, est.
20	5.2	4.7	23	0.05	0.04
50	19.5	18.9	70	1.3	1.0
60	28.6	28	94	2	1.5
80	56.9	56.9	190	5	3.5
100	103.6	105.6	250, est.	8.4	7.8

Table 2 JP-8 surrogate for modeling vaporized mixture

Name	SUPERTRAPP symbol	Formula	MW	Mass of fuel	Moles
Isooctane	224TMP	C_8H_{18}	114.229	5.00%	0.0683
Methyl cyclohexane	MCC6	C_7H_{14}	98.186	5.00%	0.07945
Meta-xylene	MXYL	C_8H_{10}	106.165	5.00%	0.07348
N-decane	C10	$C_{10}H_{22}$	142.282	15.00%	0.16449
Butyl benzene	C4BNZ	$C_{10}H_{14}$	134.218	5.00%	0.05812
N-dodecane	C12	$C_{12}H_{26}$	170.335	22.00%	0.20152
1-methylnaphthalene	1MNAPH	$C_{11}H_{10}$	142.197	10.00%	0.10972
N-tetradecane	C14	$C_{14}H_{30}$	198.388	18.00%	0.14156
N-hexadecane	C16	$C_{16}H_{34}$	226.441	15.00%	0.10335
Surrogate		$C_{11.9}H_{21.6}$	156.024	100.00%	1.00000

displace dissolved oxygen. Gaseous nitrogen was bubbled through the fuel by placing a coiled tube with small vent holes placed at the bottom of the sparging tank. Gases collected at the top of the tank were vented through a one-way valve until all dissolved oxygen was removed. Tests were performed with a gas chromatograph on air-saturated fuel to determine the amount of nitrogen to fully deoxygenate the fuels to the O_2 detection limit of the chromatograph. To further prevent the reaction between the fuel and heated metal structure, silicon-based coatings were applied to all hot section components, including the fuel nozzles.

Of the four fuels tested, the kerosene-based JP-8 used by the U.S. military was of primary interest, because the fuel has high energy density and the handling and infrastructure are readily available. JP-8 has a low vapor pressure, good for preventing accidental spills from forming a combustible mixture, but unfavorable for ease of creating a purely gaseous mixture capable of transitioning and sustaining a detonation wave. Table 1 shows a comparison of JP-8 vapor pressure with the other fuels tested. The JP-10 data are provided for comparison.

Before this work, JP-8/air detonations have been difficult to initiate and sustain because of a necessarily narrow equivalence ratio range and unsatisfactory fuel injection schemes. An incentive for this work was that of Brophy et al. [18,19] in tests with JP-10 and air, in which small fuel droplets were evaporated with a vitiated air supply (with O_2 makeup). [Single species JP-10 has a similar low vapor pressure (Table 1) to the multiple component JP-8.] Detonations were generated using a JP-10/O_2/air predetonator that channeled a developed detonation into the JP-10 and air mixture in the thrust chamber.

Flash Vaporization System

Flash vaporization, as defined here, occurs when a fuel is heated to a sufficiently high temperature that upon injection into air for precombustion mixing, vaporization occurs in the absence of heat transfer from the air, i.e., the air temperature before and after mixing with the fuel remains unchanged or is increased. The required flash vaporization temperature depends on the final pressure and temperature of the fuel/air mixture after the injection process and is not necessarily as high as the critical temperature for the fuel. In this work, fuel was pressurized above the critical pressure to prevent phase change within the system before injection. The fuel was heated to temperatures sufficient to ensure flash vaporization but below the critical temperature. Fuel nozzles were standard pressure atomization nozzles, unmodified except for the application of an ∼300 Å thick silicon coating to resist fuel coking during high-temperature injection. From photographs [10] of superheated steam injected through the nozzles, the resulting spray was shown not to impinge on the mixing duct walls.

Table 3 Minimum fuel/air mixture temperature required for 100% vapor in the intake manifold at 2 bar

Fuel	Mixture temperature, K
$n\text{-}C_7H_{16}$	287
$i\text{-}C_8H_{18}$	282
JP-8	400

Pressures in the PDE intake manifold determine whether a fuel vapor/air mixture will condense at equilibrium conditions. The amount of condensate expected in the fuel/air mixture at an equilibrium pressure and temperature can be modeled with the program SUPERTRAPP [20]. The program uses the database for thermophysical properties of hydrocarbon mixtures and computes vapor–liquid equilibrium using the Peng–Robinson model [21]. The model assumes unlimited time to reach equilibrium adiabatically. Inputs included the initial stoichiometric fuel and air enthalpies and final equilibrium pressure, in this case 2.0 bar, slightly above the maximum pressure in the actual manifold during testing. N-heptane ($n\text{-}C_7H_{16}$) and isooctane ($i\text{-}C_8H_{18}$) are single component fuels and were input as such, but JP-8 was modeled as a multicomponent fuel. Table 2 shows the 10-component surrogate mixture [10] used. The desired endpoint was 100% fuel vapor after mixing. The JP-8 surrogate model compared well to published data [22] and missed the actual JP-8/Jet A bubble point line by 12.5°C (1.84% of T_{critical}) and dew point line by 22°C (3.24% of T_{critical}). The multicomponent aviation gasoline was not modeled.

The results of the model were used to determine a fuel/air test envelope for negligible fuel droplets. Table 3 shows results for a 100% vapor mixture in the manifold at a maximum pressure of 2 bar for three fuels. For resultant fuel/air mixture temperatures at or above those in Table 3, the fuel vapor should not condense. The predicted liquid-free JP-8/air mixture temperature of 400 K compares favorably with work performed by Card et al. [23] who used similar vapor pressure (Table 1) JP-10/air and successfully produced a fully gaseous mixture at 410 K and 2 atm. For higher premixed manifold pressures, such as required to run the PDE at higher frequencies, mixture temperatures above those in Table 3 would be required.

Figures 1–3 show modeled fuel injection envelopes for a stoichiometric fuel/air mixture. The figures can be used to determine fuel and air conditions necessary for the mixture to fully evaporate or sustain a vaporized fuel without condensing. The axes are incoming fuel temperature and final mixture temperature. The horizontal line underneath the hatched box denotes the mixture temperature liquid–vapor equilibrium point from Table 3, and the air temperature lines represent the initial air temperature before mixing. The minimum flash vaporization temperature line is the locus of the intersections of equal air and mixture temperatures. Those minimums are shown in Table 4. Fuel temperatures to the left of the minimums will result in heat removed from the air to evaporate the fuel. At the flash vaporization temperatures given in Table 4, the time to change the phase of the fuel is effectively zero because no evaporation time is required. The minimum flash vaporization temperature is an important parameter in designing the length of an intake manifold for a PDE because some distance (time) will be required to mix the fuel and air sufficiently.

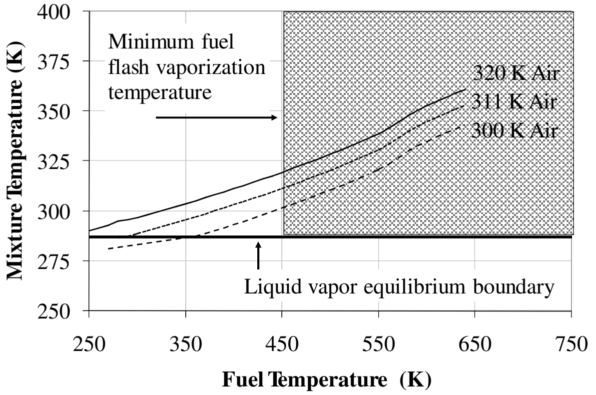

Fig. 1 Stoichiometric n-heptane–air mixture at 2 bar. Hatched region is flash vaporized.

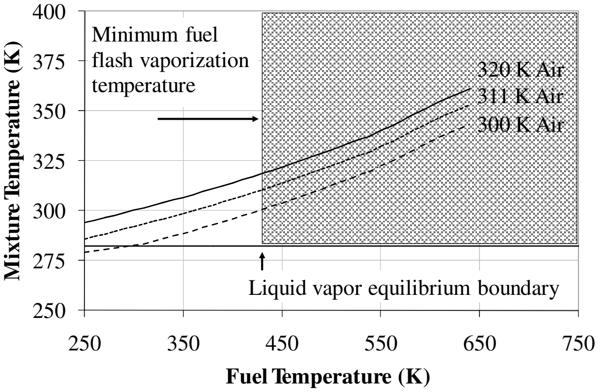

Fig. 2 Stoichiometric isooctane–air mixture at 2 bar. Hatched region is flash vaporized.

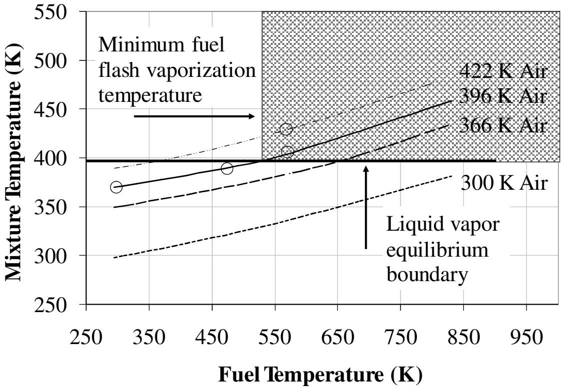

Fig. 3 Stoichiometric JP-8 surrogate–air mixture at 2 bar. Hatched region is flash vaporized.

Table 4 Minimum fuel temperature to flash vaporize for a given air temperature at 2 bar

Fuel	Air temperature, K	Fuel temperature, K
n-C_7H_{16}	311	450
i-C_8H_{18}	311	430
JP-8	422	530

Figures 1 and 2 show that high vapor pressure fuels will completely evaporate in air at relatively low fuel and air temperatures (300–320 K) without requiring flash vaporization (above the liquid–vapor equilibrium line). The low vapor pressure JP-8 surrogate (Fig. 3), however, will not completely vaporize in 300 K air without necessitating fuel temperatures well above 800 K. At temperatures above 725 K, however, the model is not reliable due to the expected endothermic reactions and the creation of smaller molecular weight species. The models indicate the benefit of heating the fuel to temperatures higher than the flash vaporization minimum for increased margin over the liquid–vapor equilibrium line.

Experimental Setup

Experiments were performed in the U.S. Air Force Research Laboratory Propulsion Directorate at Wright–Patterson Air Force Base, Ohio. The PDE is composed of a General Motors Quad 4 head with two electrically driven camshafts. The rotating cams provide a three-part cycle with equal time (120 deg) to fill, fire, and purge the thrust tubes. Up to four thrust tubes can be attached where the pistons and block would normally be, but for this research only two tubes were used. The steel tubes have a 5.25 cm inside diameter and are 152 cm in length. Firing frequency for each tube was 15 Hz for an aggregate 30 Hz, with each firing 180 deg out of phase from one another. Manifold pressure upstream of the valves was set to provide a full tube fill (fill fraction of one). The required fill mass was based on the tube volume with the fuel–air mixture at atmospheric pressure (due to the open end) and at the temperature of the mixture in the manifold upstream of the values. A more detailed explanation of the setup can be found in [1,10].

Two fuel injection locations were used. For the high vapor pressure fuels (n-heptane, isooctane, and aviation gasoline), the fuel spray bars were located 6.5 m upstream of the intake valves. The length of manifold, in conjunction with an axial mixer, provided ample time for the fuel and air to mix (Fig. 4). The 6.5 m long mixing length also improved flow quality due to the separation from largest pressure and velocity fluctuations caused by the intake valves.

For the JP-8/air mixture tests, the length from the fuel injector to the PDE tubes was reduced to 1.3 m and the axial mixer was removed (Fig. 4). This shorter mixing length challenged the performance of the flash vaporization system in two ways. First, it reduced the mixture residence time (relative to the high vapor pressure setup) from 237 to 46 ms. The reduced mixing time should exacerbate the effect of any liquid fuel by limiting the time to evaporate. Second, the fuel nozzles are now closer to the intake valves of the PDE tubes, which results in an increase in the air velocity fluctuations and pressure fluctuations. These conditions, along with the low vapor pressure of the JP-8, made this the more challenging of the two configurations.

Figure 5 shows the fuel system schematic. Not shown is a fuel pretreatment system that removed dissolved oxygen in the fuel. After deoxygenation, the fuel was loaded into a hydraulic accumulator and pressurized with gaseous nitrogen. Sufficiently high pressure near or above the critical pressure was applied to prevent phase change of the fuel during heating. After fuel heating, and with fuel and air properties at desired levels, a high-temperature-rated pneumatic ball valve was opened to allow the preheated fuel to steadily feed the fuel injection nozzles (fuel injectors). Fuel flow rates were controlled by

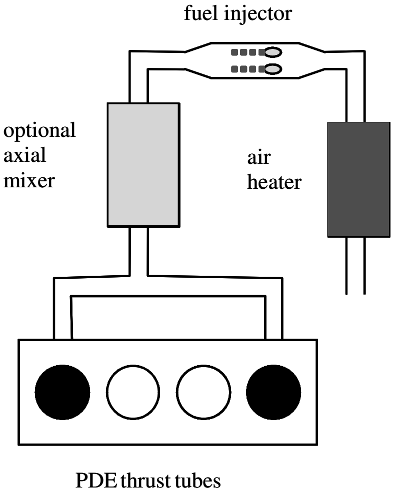

Fig. 4 Fuel/air system schematic. Filled circles represent tubes used.

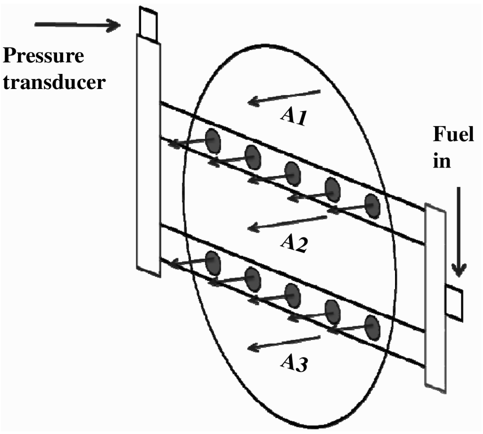

Fig. 6 Fuel injector spray bars. Circles denote fuel nozzles. Arrows show fuel and air flow direction.

nitrogen bottle pressure and by varying the number and size of the atomization nozzles. Downstream, the fuel/air mixture traveled to the intake manifold and was intermittently fed at the cycle frequency into the two thrust tubes for combustion. Run times of up to 2 min were possible before exhausting stored heated fuel. This process was repeated until the deoxygenated fuel stored in the accumulator was consumed.

The fuel was injected tangentially with the air flow with two spray bars (Figs. 4 and 6). Standard pressure atomization nozzles were used. The fuel injector pressure and temperature were recorded during testing. In Fig. 6, the area between the spray bars and the manifold walls (A1, A2, and A3) are equal and thus allow roughly equal air flow around the injectors. The four nozzles closest to the walls were not used during this work.

The dual spray bar depicted in Fig. 6 allowed nozzle sizing for a variety of fuel temperatures and fuel flow rates. Ten fuel pressure atomization nozzles could be used in combinations of nozzle flow numbers (FN) to match the desired flow rate using the relationship [24]

$$\mathrm{FN} = \frac{\dot{m}}{\sqrt{\Delta P}} \tag{1}$$

where $\dot{m}$ is mass flow (lbm/h) and ΔP is the pressure drop across the nozzle (psi). The flow numbers are additive and allow the use of several nozzles to match the desired flow rate. For increased fuel temperatures, the density decreases (Figs. 7 and 8) and Eq. (1) must be corrected:

$$\mathrm{FN} = \frac{\dot{m}}{\sqrt{\Delta P}} \sqrt{\frac{\rho_{\mathrm{cal}}}{\rho_{\mathrm{actual}}}} \tag{2}$$

where ρ_{cal} is the nozzle calibration density (768.9 $\mathrm{kg/m^3}$) and ρ_{actual} is the density as given by Figs. 7 and 8. As seen in the figures, above the critical temperature, density depends on both temperature and pressure. Any combination of the nozzles given in Table 5 was used to match the desired fuel flow rate at the preset injection temperature; however, the actual fuel flow rate was measured directly using a calibrated turbine flow meter, as shown in Fig. 5.

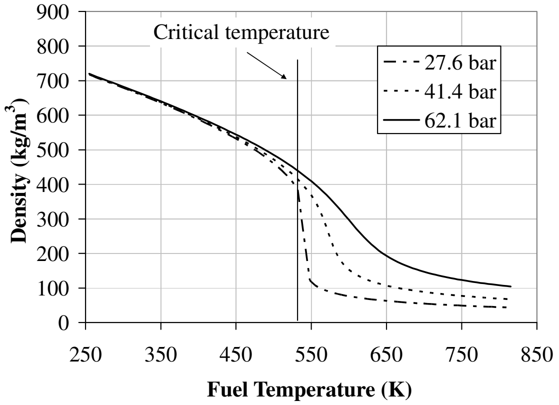

Fig. 7 Heptane density for three pressures. The vertical line denotes the critical temperature.

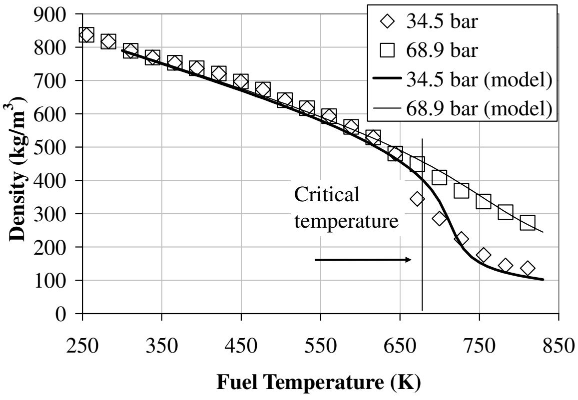

Fig. 8 Comparison of modeled JP-8 surrogate with experimental data from [31].

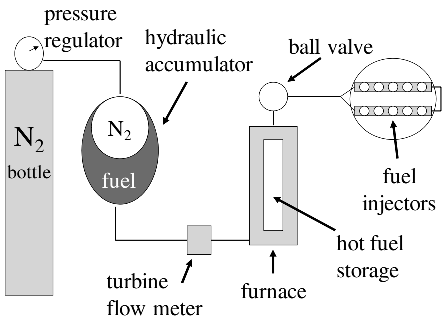

Fig. 5 High pressure fuel system schematic.

Droplets generated by a pressure atomization nozzle are characterized by mean drop size, drop size distribution, spray pattern, and spray cone angle. The definition of mean diameter varies depending on its intended use. The Sauter mean diameter (SMD) is used to describe a characteristic droplet with a volume-to-surface ratio equal to that of the spray as a whole. The SMD performance for a representative pressure atomization nozzle with a flow number of 1.1 produced droplets between 23 and 67 μm using unheated fuel and a pressure differential of 6.9 bar.[§]

Table 5 Delevan pressure atomization nozzles used for PDE fuel injection§

Fuel nozzle, P/N	Test pressure, psid	Flow limits, lbm/h		Spray angle, deg	Flow no.
		High	Low		
27710 - 18	100	4.2	3.8	90	0.4
46817 - 4	100	5.3	4.7	70	0.5
59216 - 5	100	10.4	9.6	90	1.0
27700 - 17	100	9.9	9.6	82.5	1.0
27700 - 18	100	9.9	9.6	62.5	1.0
27710 - 8	100	16.4	15.6	75	1.6

Figure 9 is a schematic of a PDE thrust tube instrumented for measuring head pressure, wave speeds, and combustion wave spiral transit time. The pressure rise in the head (closed end) of the PDE was used to determine ignition onset. The pressure was measured by a dynamic PCB-Piezotronics ICP pressure transducer. Combustion wave speeds were captured by ion probes used as time of flight sensors. The ion probes were located near the end of the tube, forward and aft of the end of the spiral. The wave speeds shown in the results section are determined by the measured time for the wave to travel between probes 2 and 3. The spiral length was kept constant for all four fuels tested.

A 12 V dc automotive digital ignition system powered the spark plug used to initiate combustion. The system provided three 250 μs duration 105–115 mJ sparks [25] every 1.1 ms (+/ − 37 μs) into the fuel and air mixture via a capacitive discharge.

Results

The performance of the FVS was evaluated by comparing the combustion performance of fuels at ambient temperature to those heated to temperatures up to and above the flash vaporization temperatures shown in Table 4. All experimental data were taken after the fuel flow rate and fuel temperature had reached steady state ($\sim$300 cycles) and was not observed to change more than 2–4% during an individual run. Three combustion parameters were examined. First was the time for a combustion wave to exit the spiral at probe 2 after spark deposition in the closed end of the tube. This time is important in establishing the overall cycle period of a PDE tube, which ultimately determines thrust density. Second was the combustion wave speed between probes 2 and 3, which determines whether or not a detonation was achieved. A detonation was considered to have occurred if the measured wave speeds were within ±10% of the theoretical Chapman–Jouguet (CJ) wave speed. The third variable was the time after ignition required for the combustion wave to exit the spiral. This represents the time required to transition the deflagration into a detonation. Ignition time was determined by the pressure rise rate in the closed end of the PDE thrust tube during the firing cycle. When the rate of pressure increase (kPa/s) was five times larger than the maximum rate observed without combustion, then ignition was said to have occurred [10]. The value is roughly half the peak pressure rate observed during testing, and this method desensitizes the data reduction to any temperature shift in the pressure transducer or variation from sensor to sensor.

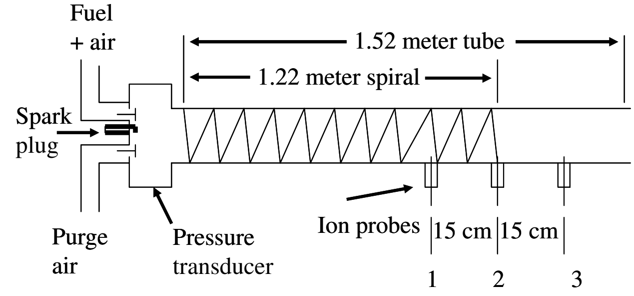

Fig. 9 Instrumentation on a single PDE thrust tube.

Results are presented in two sections. The first section contains the three high vapor pressure fuels (n-heptane, isooctane, and aviation gasoline) and represents cases with the highest likelihood of droplet-free fuel and combustion, due in part to the long mixing length (6.5 m). As shown in Figs. 1 and 2, and giving sufficient time for the fuel and air mixture to reach equilibrium, fuels at ambient temperature will completely evaporate in 311 K air. The aviation gasoline was not modeled but has a vapor pressure three to four times that of isooctane (Table 1) and should evaporate even more quickly. The second section presents combustion data of the vaporization of low vapor pressure JP-8. This was the more difficult case due to the shorter mixing length (1.3 m) and higher air and fuel temperatures required to elevate the mixture temperature above the liquid–vapor equilibrium line (Fig. 3).

The maximum allowable combustion times for this work were limited by the mechanical setup and the firing frequency. At a 15 Hz firing frequency for this experimental setup, the total cycle time is 66.6 ms with equal time (22.2 ms) allowed to fill, fire, and purge the PDE tube. The 22.2 ms available to the fire portion of the cycle must allot time for the spark delay, spark deposit, ignition of the fuel, transition of the deflagration into a detonation, and exhaustion of the high pressure gases (blow down) before beginning the purge portion of the cycle. The gas dynamics of the mixture, during the filling of the long slender PDE tube from the closed end, requires an 8 ms spark delay to avoid igniting the fuel and air mixture in the low pressure region caused by an expansion wave immediately after the intake valve closes. The 8 ms spark delay provided an average total pressure of 1.05 bar in the closed end of the thrust tube during the ignition portion of the fire cycle. Additionally, the PDE thrust tube required roughly 4 ms to exhaust the high pressure products, leaving only about 10 ms to ignite and detonate the mixture. Many runs had measured ignition times over 10 ms, resulting in high-pressure hot combustion products remaining in the thrust tube when the purge manifold valves opened. In extreme cases, insufficient purge occurred and the incoming fuel and air mixture for the next cycle was ignited by the hot combustion products from the previous cycle instead of the desired spark ignition. Such ill-timed combustion waves can travel into the intake manifold during the fill process and potentially damage the PDE. In all cases that follow, data points are averages of eight combustion events and error bars are ±1 standard deviation.

High Vapor Pressure Fuel/Air

Figures 10 and 11 show the time from spark deposition in the closed end of the PDE tube to a combustion wave being observed at the second ion probe for the three high vapor pressure fuels. Fuel temperatures ranged from ambient to 500 K. Solid and dashed lines are second-order polynomial curve fits of the data. The figure contains both unheated and heated flash vaporized fuels. Because no dependence on the fuel injection temperature was observed, the combined ambient and heated fuel data sets were plotted without temperature delineation. It appears that a richer mixture favors lower combined ignition and detonation time, but, as will be shown later, combustion wave speeds will decrease at a higher equivalence ratio φ. The equivalence ratio is given by the following relationship

$$\phi = \frac{(\text{fuel/air})_{\text{actual}}}{(\text{fuel/air})_{\text{stoich}}} \tag{3}$$

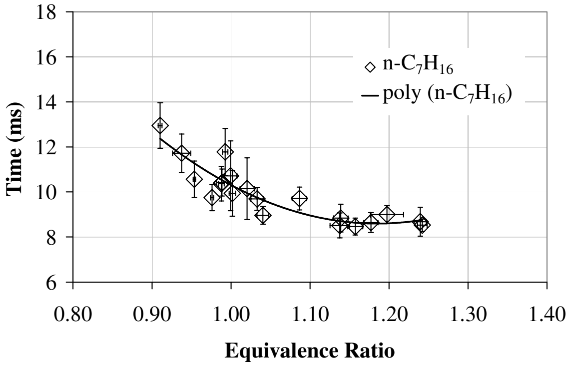

Fig. 10 Total time from spark deposit to combustion wave arrival at probe 2 for n-heptane and air.

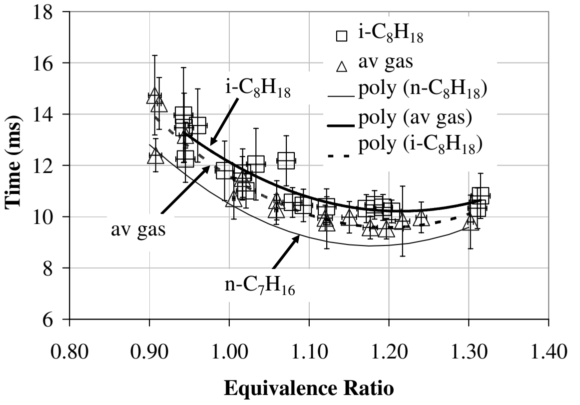

Fig. 11 Total time from spark deposit to combustion wave arrival at probe 2 for three high vapor pressure fuels with air.

where fuel and air can be defined by mass, mole/volume, partial pressure, or mole fraction in the mixture. Stoichiometric ($\varphi = 1$) is defined as the ratio of fuel and oxygen that is completely balanced due to conservation of atomic species, and theoretically result in no excess fuel or oxygen in the combustion products. Although water and carbon dioxide are the primary products for hydrocarbon combustion, small amounts of other species are also produced in a real combustion event. If the ratio is less than stoichiometric ($\varphi < 1$) then the mixture is fuel lean, and if the mixture is greater than stoichiometric ($\varphi > 1$) then the mixture is fuel rich. In Figs. 10 and 11, at a φ of 1, the isooctane takes roughly 12 ms to transit the spiral, 1 ms more than the aviation gasoline and 2 ms more than the n-heptane.

The combustion wave speed measured between probes 2 and 3 determines whether a detonation wave was achieved. Figure 12 shows combustion wave speeds for the high vapor pressure fuels compared with the predicted CJ wave speeds from Gordon and McBride's Chemical Equilibrium with Applications (CEA) program [26]. Again, no fuel temperature dependence was observed. Larger standard deviations are observed at lean and rich limits (i.e., the detonation limits), especially for the isooctane, due to the difficulty in obtaining detonations at those conditions. The isooctane also has the narrowest equivalence ratio range of detonation occurrence ($0.95 < \varphi < 1.2$). The n-heptane and aviation gasoline both achieved detonations for the entire range of equivalence ratios tested (0.9–1.3).

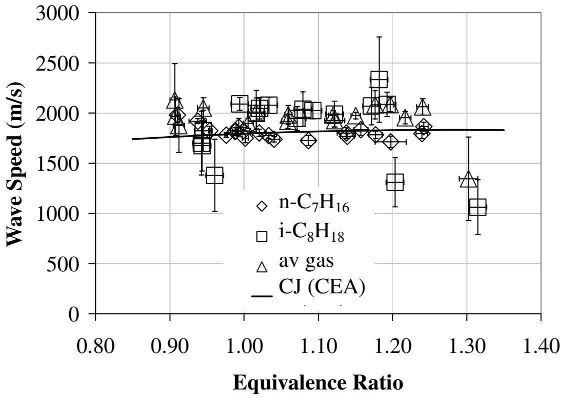

Fig. 12 Average wave speeds between probes 2 and 3 for three high vapor pressure fuels.

In Fig. 12, n-heptane agrees best with the predicted CJ velocities. This is most likely due to an earlier transition from a deflagration to a detonation and the wave relaxing to the steady-state CJ speed. Panzenhagen et al. [27] found, in a similar setup, that the detonation transitioned at roughly 1 m of spiral. The aviation gasoline and isooctane most likely transitioned later and had not yet reached the steady-state velocity at the end of the 1.22 m spiral used in this work. During the transition process, using an obstacle such as a Schelkin spiral, the detonation velocity will often overshoot the CJ velocity before reaching steady state.

The detonability limits of the mixtures fall within equivalence ratio bounds for gaseous normal alkane fuels with a high explosive (HE) initiator [28] (see Table 6). The range of equivalence ratios that can sustain a detonation is narrow compared with the combustion limits, and, although the detonation initiation method in Fig. 11 differs, the combustion results fall near the 1 MJ HE initiation energy values in Table 6.

Early in this work, detonation transition was attempted with a 0.914 m spiral. Stoichiometric n-heptane/air was successful, but stoichiometric isooctane/air was not, again suggesting the earlier transition for n-heptane mentioned previously. For a spiral length of 1.22 m, however, isooctane/air detonations were successfully transitioned but at a more narrow equivalence ratio range. Typically, longer spirals extend the useful equivalence ratio range, but at a cost of extra weight and internal drag. The distance to transition a detonation sets the minimum PDE thrust tube length when using this type of DDT mechanism.

Time to transition a deflagration into a detonation was a third parameter of interest. This is defined as the time from an initial combustion-driven pressure rise in the closed end of the tube to the arrival of the combustion wave at probe 2. This time is, in effect, the spiral transit time and is shown in Fig. 13. Again, no fuel temperature dependence was observed. Although the time data do not indicate whether a detonation occurred, detonations correlate with shorter times due to the higher speed of the combustion wave. Several important features stand out in Fig. 13. The first is that measured times are lowest near an equivalence ratio of 1. This suggests that the minimum detonation initiation energy for these hydrocarbon fuels occurs at or slightly richer (5–10%) than the stoichiometric equivalence ratio. The minimum detonation energy also corresponds to where most hydrocarbon/air detonation cell sizes are the smallest [17,28,29]. Likewise, Card et al. [23] noted the minimum measured detonation run-up distance for several hydrocarbon/air mixtures at

Table 6 Detonation equivalence ratio limits for gaseous hydrocarbon fuels in air at 293 K and 1 atm

Fuel	Formula	1 MJ lean limit φ_L	1 MJ rich limit φ_R	Max lean limit φ_L	Max rich limit φ_R
Ethane	C_2H_6	0.81	1.65	0.69	2.00
Propane	C_3H_8	0.93	1.45	0.70	1.90
N-butane	n-C_4H_{10}	0.88	1.50	0.70	2.03

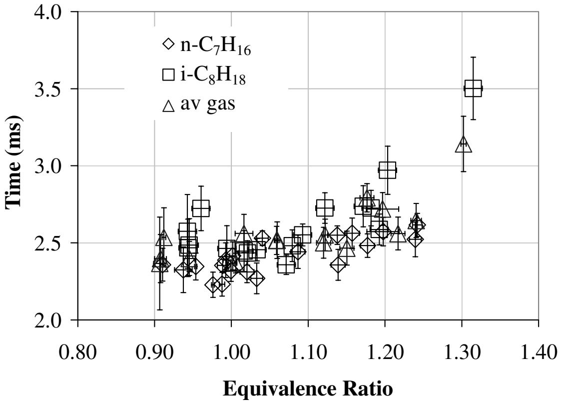

Fig. 13 Spiral transit time for three high vapor pressure fuels.

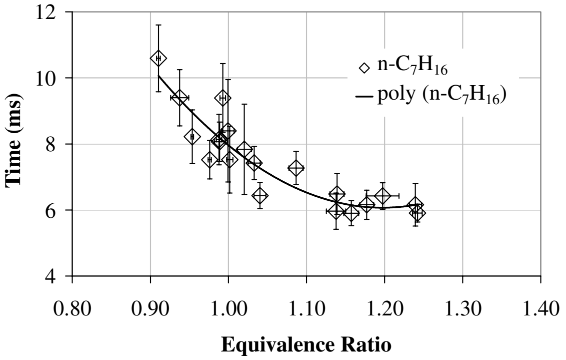

Fig. 14 Time from spark deposit to initial pressure rise in the closed end of the PDE tube (ignition time) for n-heptane and air.

equivalence ratios of approximately 1.05–1.2 and corresponded to where the mixture laminar flame speed was a maximum. The lower detonation initiation energy near a stoichiometric equivalence ratio might correlate to a detonation transitioning faster for a fixed initiation energy (and obstacle length) and therefore take the least amount of time to traverse the spiral. The n-heptane was the fastest to transition a detonation and isooctane was the slowest. Most of detonations were observed at transition times on the order of 2.6 ms or less. At longer times, detonations, as defined by wave speed, did not occur.

The distribution of the data in Fig. 13 is also of interest. When compared with total combustion time in Figs. 10 and 11, the spiral transit time is much flatter over the range of equivalence ratios. Both the shape of the curve and the magnitude of the error bars in Fig. 11 are dominated by the time for the initial pressure rise in the closed end of the head, defined as ignition time and shown in Fig. 14. The time for the combustion wave to transit the spiral (Fig. 13) is only about one-fourth of the time that is needed to generate ignition (Fig. 14). The reduction of ignition time is a more relevant step in reducing the time required to initiate a detonation using a similar obstacle method.

In all the previous results, the absence of fuel injection temperature dependence implies an absence of liquid droplets. The fuel injection envelope predictions (Figs. 1 and 2) support the assumption that given adequate time (or mixing length), ambient temperature isooctane mixed with air at 311 K will achieve 100% vapor based on the total enthalpy of the mixture (-6060 kJ/kg), which corresponds to a 292 K mixture temperature, well above the liquid–vapor equilibrium line (Fig. 2).

Low Vapor Pressure JP-8/Air

JP-8 combustion results were strongly influenced by the fuel injection temperature and are shown in Fig. 15. The data are presented at two air temperatures and at four fuel temperatures: two above and two below the expected flash vaporization temperature of 530 K (Table 4). These operating conditions were identified earlier in the predicted flash vaporization test envelope and indicated by the circles in Fig. 3. The flash vaporized fuel (denoted by the triangles and circles in Fig. 15) exhibited lower ignition times and achieved ignition at leaner equivalence ratios. The effect of the droplets on the total time to achieve the desired detonation wave at φ of 1 is observed to increase from 10 to 14 ms.

Mixtures with fuel injection temperatures below the flash vaporization temperature did not achieve ignition within the required time restraints of the current cycle ($\sim$12 ms) until the mixtures reached or exceeded equivalence ratios of 0.98 for the 465 K fuel and 1.08 for the 307 K fuel. This is likely due to remaining liquid fuel lacking sufficient time to evaporate before combustion. In effect, remaining droplets are not available for combustion within the allotted time scales. Thus, only the fuel already in vapor form was available for combustion. One can see this from the best fit lines from Fig. 15 replotted in Fig. 16. The unheated (307 K) JP-8 line has the same shape as the flash vaporized line but appears shifted to the right (fuel rich) by an increase in equivalence ratio of 0.15. This infers that 15% more fuel was required to reach a mixture that behaved as the fully vaporized mixture. Globally, the mixture was fuel rich, but, locally, the remaining liquid fuel did not contribute to the detonation initiation process, effectively making the local mixture leaner.

Figure 17 shows spiral transit time, the time from initial pressure rise in the closed end of the tube to the combustion wave arrival at probe 2, for various equivalence ratios and fuel temperatures. The spiral transit time was relatively independent of fuel temperature. The primary effect of the JP-8 fuel temperature was on the minimum lean ignition limit. It is believed that any remaining fuel droplets did not contribute to the combustion and only the fuel vapor available and generated by the passing detonation participated. The circled temperatures in Fig. 17 denote the leanest φ for ignition for three fuel temperatures, given the 22 ms time limit on the fire phase of the cycle.

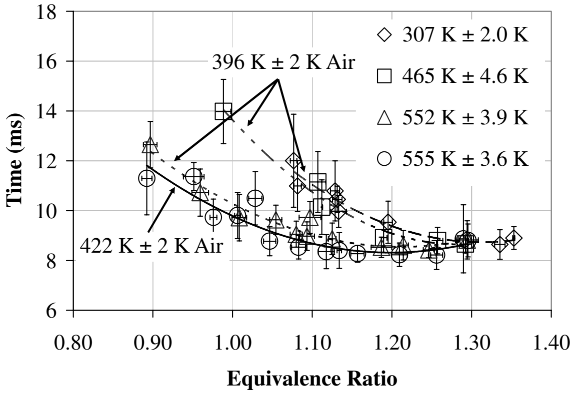

Fig. 15 Total time from spark deposit to combustion wave arrival at probe 2 for JP-8 and air.

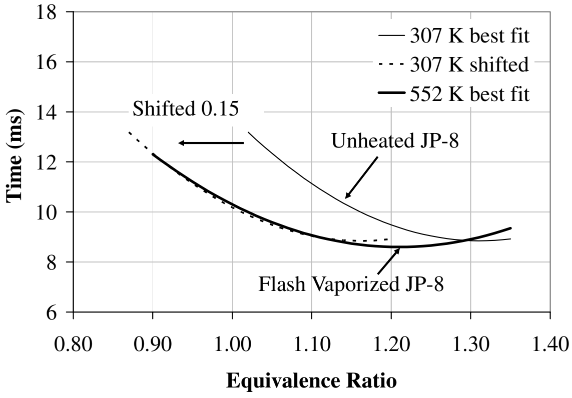

Fig. 16 Best fit lines for total time from spark deposit to combustion wave arrival at probe 2 for JP-8 and 394 K air.

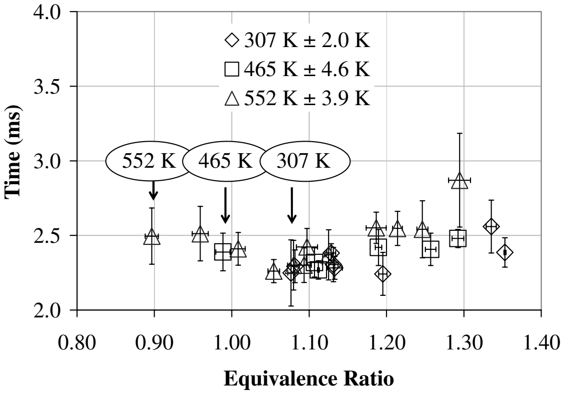

Fig. 17 Spiral transit time for JP-8 and air at three fuel temperatures into 396 K (±2 K) air. The ovals denote the leanest mixture where ignition was achieved for each fuel temperature.

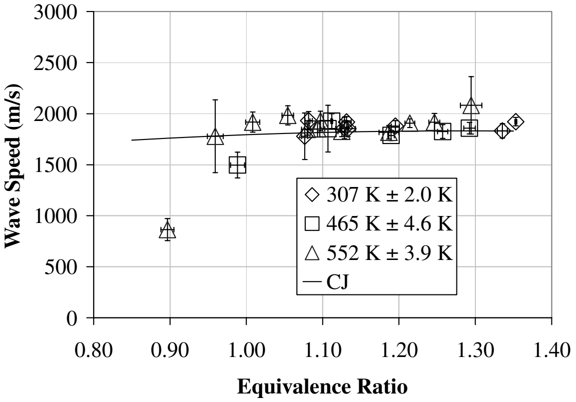

Fig. 18 Average combustion wave speed between sensors 2 and 3 for three fuel temperatures into 396 K air.

For example, the 307 K fuel temperature could not operate leaner than a φ of 1.08, whereas the lean limit at 552 K was 0.89. Similar to the earlier high vapor pressure fuels, flash vaporized JP-8 reaches a minimum spiral transit time at a φ of 1.05, which correlates well with the minimum detonation initiation energy required for that mixture condition.

Wave speeds for JP-8/air mixtures detonated with (552 K case) and without (307 and 465 K) full flash vaporization are shown in Fig. 18 and agree well with the predicted CJ results. The two lower temperature fuels, presumably containing liquid droplets (refer to Fig. 3), required a considerably richer mixture than the flash vaporized case to achieve detonation and CJ speed. Like the high vapor pressure fuels, the detonation wave speed standard deviations increase for the leaner and richer detonability limits. The flash vaporized JP-8 detonability range was 0.90–0.95 at the lean limit and greater than 1.3 (1.3 was the highest tested) at the rich limit.

Conclusions

This is the first reported successful effort to flash vaporize and detonate a wide variety of liquid hydrocarbon fuels with air, including the low vapor pressure JP-8, in a working pulsed detonation engine. Detonations were achieved over a wide operating equivalence ratio, without oxygen enhancement or a predetonator. Fuel injection temperature had no measurable influence on the combustion for the aviation gasoline, i-C_8H_{18}, and n-C_7H_{16} due to both the high vapor pressure of the fuels as well as the long mixing length between the fuel injectors and the PDE thrust tubes. Low vapor pressure JP-8 droplets delayed ignition and DDT times for a given equivalence ratio vs fully vaporized fuel mixtures. Remaining fuel droplets did not contribute to ignition, and the mixture was effectively leaner. For JP-8 fuel at temperatures that insured flash vaporization (>530 K), the combustion data collapse to near that of the performance of the high vapor pressure n-heptane.

The FVS reduced the lean operating ignition limit from an equivalence ratio of 1.08 with ambient temperature fuel to a value of 0.89 with the 555 K fuel. In agreement with other liquid-fueled PDE studies [9,18], the larger the percentage of the fuel in the vapor state, the better the overall performance of the PDE.

The practicality of a flash vaporization system was also evaluated. The FVS enabled the low vapor pressure JP-8 to have comparable ignition and detonation results relative to the high vapor pressure fuels, even with a much shorter mixing length. This method eliminated the effects of fuel droplets and mimics a gaseous-fueled operation of a PDE. Likewise, the fuel preparation techniques validated the ability to safely heat fuel to temperatures over 330°C without thermal-oxidative and endothermic reactions damaging the fuel system, which has prevented implementation on realistic systems in the past. Subsequent work [30] has proved the applicability of flash vaporization as a reliable method to detonate a variety of low vapor pressure jet fuels.

The conditions required to successfully flash vaporize and achieve a mixture without droplets were accurately modeled. The JP-8 and air modeling showed that for 300 K fuel and 422 K air at a manifold pressure of 2 bar, the enthalpy available in the fuel and air was insufficient to completely evaporate the fuel. Likewise, for 300 K air, no fuel temperature short of 850 K could sufficiently ensure complete fuel vaporization. At these fuel temperatures, pyrolytic reactions begin to occur in the fuel and the liquid/vapor equilibrium code does not capture the expected endothermic reactions and thus would not accurately predict mixture states. Fuel breakdown kinetics become significant at these higher fuel injection temperatures [13,14].

Acknowledgments

The authors thank Royce Bradley, Curt Rice, John Hoke, Kristin Panzenhagen, Jeff Stutrud, and Tim Edwards for their valuable help and hard work. This work was funded by the U.S. Air Force Research Laboratory's Propulsion Directorate and the U.S. Air Force Office of Scientific Research. The views expressed in this paper are those of the authors and do not reflect the official policy or position of the U.S. Air Force, the Department of Defense, or the U.S. Government.

References

[1] Schauer, F., Stutrud, J., and Bradley, R., "Detonation Initiation Studies and Performance Results for Pulsed Detonation Engine Applications," *39th AIAA Aerospace Sciences Meeting & Exhibit*, AIAA Paper 2001-1129, Jan. 2001.

[2] Roy, G. D., "Pulsed Detonation Phenomena for Air Breathing Propulsion," *14th International Symposium of Air Breathing Engines*, International Symposium of Air Breathing Engines 1999-7127, Sept. 1999.

[3] Kailasanath, K., "Review of Propulsion Applications of Detonation Waves," *AIAA Journal*, Vol. 38, No. 9, Sept. 2000, pp. 1698–1708.

[4] Balla, D. R., and Lefebvre, A. H., "Ignition and Flame Quenching of Quiescent Fuel Mists," *Proceedings of the Royal Society of London, Series A: Mathematical and Physical Sciences*, Vol. 364, No. 1717, 1978, pp. 277–294.
doi:10.1098/rspa.1978.0201

[5] Bar-Or, R., Sichel, M., and Nicholls, J. A., "Reaction Zone Structure of Cylindrical Detonations in Monodisperse Sprays," *Nineteenth Symposium (International) on Combustion*, Combustion Inst., Pittsburgh, PA, 1982, pp. 665–673.

[6] Lin, Z. C., Nicholls, J. A., Tang. M. J., Kauffman, C. W., and Sichel, M., "Vapor Pressure and Sensitization Effects in Detonation of a Decane Spray," *Twentieth Symposium (International) on Combustion*, Combustion Inst., Pittsburgh, PA, 1984, pp. 1709–1716.

[7] Dabora, E. K., Ragland, K. W., and Nicholls, J. A., "Droplet-Size Effects in Spray Detonations," *Twelfth Symposium (International) on Combustion*, Combustion Inst., Pittsburgh, PA, 1969.

[8] Bar-Or, R., Sichel, M., and Nicholls, J. A., "Propagation of Cylindrical Detonations in Monodisperse Sprays," *Eighteenth Symposium (International) on Combustion*, Combustion Inst., Pittsburgh, PA, 1981, pp. 1599–1606.

[9] Kailasanath, K., "Liquid-Fueled Detonations in Tubes," *Journal of*

Propulsion and Power, Vol. 22, No. 6, 2006, pp. 1261–1268. doi:10.2514/1.19624

[10] Tucker, K. C., "Flash Vaporization System for Detonation of Hydrocarbon Fuels in a Pulse Detonation Engine," Ph.D. Dissertation, Graduate School of Engineering and Management, Air Force Inst. of Technology (AU), Wright–Patterson AFB, OH, June 2005.

[11] Lefebvre, A. H., *Gas Turbine Combustion*, Taylor and Francis, Philadelphia, 1999.

[12] Ervin, J. S., Williams, T. F., and Hartman, G., "Effect of Test Period on the Rate of Fouling in a Complex Flowing System," *Structure of Jet Fuels V*, Vol. 43, No. 3, American Chemical Society, Washington, D.C., Aug. 1998, pp. 373–377.

[13] Yoon, E. M., Selvaraj, L., Eser, S., and Coleman, M. M., "High-Temperature Stabilizers for Jet Fuels and Similar Hydrocarbon Mixtures, 2: Kinetic Studies," *Energy and Fuels*, Vol. 10, No. 3, 1996, pp. 812–815.

[14] Ward, T. A., Ervin, J. S., Striebich, R. C., and Zabarnick, S., "Simulations of Flowing Mildly-Cracked Normal Alkanes Incorporating Proportional Distributions," *Journal of Propulsion and Power*, Vol. 20, No. 3, 2004, pp. 394–402. doi:10.2514/1.10380

[15] *Handbook of Aviation Fuel Properties/CRC*, 2nd Printing, Coordinating Research Council, Atlanta, Rept. No. 53, May 1984.

[16] Yaws, C. L., *Chemical Properties Handbook*, McGraw–Hill, New York, 1999.

[17] Austin, J. M., and Shepherd, J. E., "Detonations in Hydrocarbon Fuel Blends," *Combustion and Flame*, Vol. 132, Nos. 1–2, 2003, pp. 73–90. doi:10.1016/S0010-2180(02)00422-4

[18] Brophy, C. M., Netzer, D. W., and Sinibaldi, J., "Operation of a JP-10/Air Pulse Detonation Engine," *36th AIAA/ASME/SAE/ASEE Joint Propulsion Conference*, AIAA Paper 2000-3591, Huntsville, AL, 16–19 July 2000.

[19] Brophy, C., Netzer, D., and Forster, D., "Detonation Studies of JP-10 with Oxygen and Air for Pulse Detonation Engine Development," *34th AIAA/ASME/SAE/ASEE Joint Propulsion Conference*, AIAA Paper 98-4003, July 1998.

[20] Huber, M. L., "National Institute of Standards and Technology Thermophysical Properties of Hydrocarbon Mixtures Database (SUPERTRAPP) Ver. 3.1 Users' Guide," U.S. Dept. of Commerce, Feb. 2003.

[21] Peng, D. Y., and Robinson, D. B., "New Two-Constant Equation of State," *Industrial and Engineering Chemistry Fundamentals*, Vol. 15, No. 1, 1976, pp. 59–64. doi:10.1021/i160057a011

[22] Szetela, E. J., and TeVelde, J. A., "External Fuel Vaporization Study, Phase 2 Final Report," NASA, CR 165513, Nov. 1981.

[23] Card, J., Rival, D., and Ciccarelli, G., "DDT in Fuel-Air Mixtures at Elevated Temperatures and Pressures," *Shock Waves*, Vol. 14, No. 3, 2005, pp. 167–173. doi:10.1007/s00193-005-0260-y

[24] Lefebvre, A. H., "Fuel Atomization, Droplet Evaporation, and Spray Combustion," *Fossil Fuel Combustion, A Source Book*, Wiley, New York, 1991.

[25] "MSD® Digital DIS-4 Ignition System Installation Instructions," Autotronic Controls Corp., El Paso, TX, 2000.

[26] Gordon, S., and McBride, B., "Computer Program for Calculation of Complex Chemical Equilibrium Compositions and Applications," NASA RP 1311 1 & 2, Oct. 1994, June 1996.

[27] Panzenhagen, K. L., King, P. I., Tucker, K. C., and Schauer, F. R., "Liquid Hydrocarbon Detonation Branching in a Pulse Detonation Engine," *40th AIAA/ASME/ASEE Joint Propulsion Conference and Exhibit*, AIAA Paper 2004-3401, July 2004.

[28] Kaneshige, M., and Shepherd, J. E., "Detonation Database," California Inst. of Technology, Graduate Aeronautical Lab. TR FM97-8, July 1997.

[29] Ciccarelli, G., and Card, J., "Detonation in Mixtures of JP-10 and Air," *AIAA Journal*, Vol. 44, No. 2, 2006, pp. 362–367. doi:10.2514/1.18582

[30] Helfrich, T. M., King, P. I., Hoke, J. L., and Schauer, F. R., "Effect of Supercritical Fuel Injection on the Cycle Performance of a Pulsed Detonation Engine," *Journal of Propulsion and Power*, Vol. 23, No. 4, 2007, pp. 748–755. doi:10.2514/1.26551

[31] Faith, L. E., Ackerman, G. H., and Henderson, H. T., "Heat Sink Capabilities of Jet A Fuel: Heat Transfer and Coking Studies," NASA CR-72951, July 1971.

J. Powers
Associate Editor